Assessing road pavement quality based on opportunistic in-car sound and vibration monitoring

26th INTERNATIONAL CONGRESS ON SOUND AND VIBRATION
7-11 July 2019, Montreal

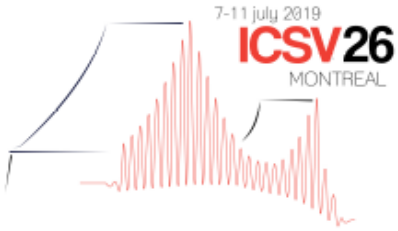

ASSESSING ROAD PAVEMENT QUALITY BASED ON OPPORTUNISTIC IN-CAR SOUND AND VIBRATION MONITORING

Wout Van Hauwermeiren, Joachim David, Luc Dekoninck, Toon De Pessemier, Wout Joseph, Dick Botteldooren and Luc Martens
WAVES, Department of Information Technology, Ghent University, Gent, Belgium

Karlo Filipan and Bert De Coensel
ASAsense cvba, Brugge, Belgium

The quality of road pavements influences noise and vibration emissions caused by tire-road interactions. This affects the drivers, passengers and load but also health and well-being of residents near these roads. Road pavement quality degrades over time due to wear, accidents, and infrastructure works. Monitoring road pavement state can rely on dedicated vehicles equipped with a CPX trailer (Close-Proximity method) or with laser texture scanning. However, using this approach, it remains difficult to cover the whole road infrastructure network at regular intervals. In this paper, an opportunistic approach is proposed: equipping cars that are on the road for other purposes with noise and vibration sensors. This way, personnel costs are avoided, and timeliness of the information could be increased. The proposed method collects spectral sound and vibration data from a sensor box placed near the rear wheel of the car. These data are transmitted over 3G to a central server. The box is also equipped with a GPS tracker that allows locating the vehicles on a road map and deriving their driving speed. Data analytics accounts for modifiers such as the driving speed and the transfer function between the tire and the microphone. Features related to the roughness of the pavement are extracted and the abundance of data is used to eliminate confounders such as the engine noise and vibrations, other cars and trucks driving near the sensor box, or music and voices. The resulting texture indicators for each 20-meter road segment correlate very well to CPX and laser texture measurements. The difference between worn-out roads (>15 years) and new pavements (<5 years) is statistically significant.
Keywords: rolling noise and vibrations, pavement, monitoring

1. Introduction

Rolling noise is caused by the complex interaction of tires with the pavement [1]: macro texture interacts with the tire groves reducing or increasing air-pumping effects while mega texture causes tire vibrations. Car vibrations at the other hand are determined by waviness and irregularity of the road surface [2]. Both noise and vibrations limit comfort of the driver and passengers. Strong vibrations may even cause cargo damage. Sound and vibration also affect health and well-being of the residents near the roads [3]. Hence, an appropriate choice of pavement should be made when new roads are constructed. However, road surfaces degrade over time and thus also a timely maintenance is required to keep noise and vibrations within limits. Road administrators therefore use standardized measurement methods to monitor this degradation (see Section 2). However, such methods (CPX, laser scanning) are time consuming and require specialized equipment. Hence, it is difficult to cover all roads in a timely manner.

In this paper, an opportunistic sensing approach is presented to assess pavement degradation more efficiently and with much more spatial coverage. Previous research has introduced similar approaches, such as Roadroid [4], which uses accelerometer data from smartphones attached to the dashboard of

vehicles, or SENSOVO [5], which uses dashboard cameras and accelerometers placed in regular vehicles. Similarly, our proposed opportunistic approach is minimally invasive, while focusing on data quality. To this end, a fleet of cars is equipped with a sensor box which is continuously monitoring sound and vibrations inside the trunk of the car. Opportunistic measurement, however, faces several confounders and modifiers (Fig. 1) that must be removed by exploring the abundancy of the acquired data. In previous work, we used the same opportunistic sensing to label road surfaces according to their noisiness [6].

This paper starts by reviewing standards for pavement quality. Then, a simple model relating road texture to sound and vibration, is presented. Finally, results from a pilot project showing that the system is capable of distinguishing different roads and degradation, is discussed.

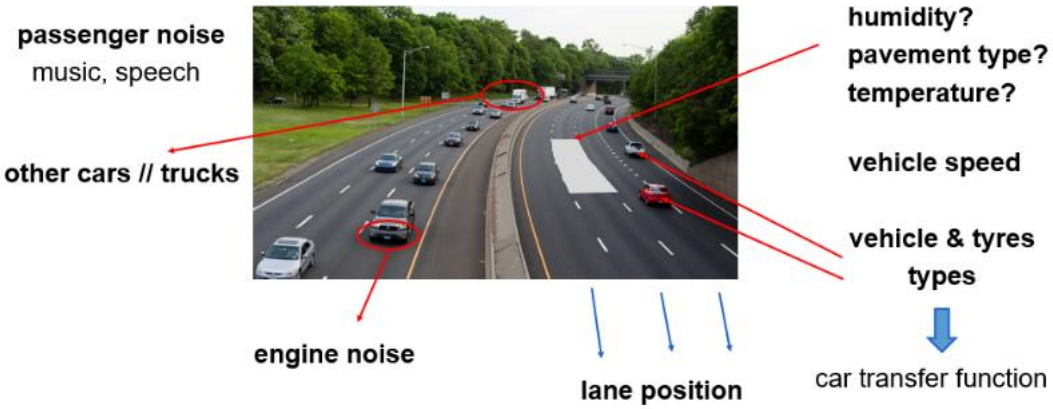

Figure 1: Confounders and modifiers that need to be accounted for in the opportunistic monitoring of the road pavement quality.

2. Quality indicators for road pavement texture

Road texture is defined as “deviation of a pavement surface from a true planar surface”. Road texture is classified according to its spatial, i.e. longitudinal wavelength. Standard ISO 10844:2014 [7] defines micro texture, macro texture, mega texture and irregularity (

). In this paper, we focus on the 5cm to 10m range (mega texture and irregularity). In every texture band, several road features account for the amplitude of the texture (such as the aggregate, binder, potholes, etc.). The longitudinal road profile can be measured accurately using laser texture measurements [8].

Table 1: Overview of the road texture classification according to ISO 10844:2014 [7].

	Spatial wavelength range	Common amplitude range	Road features	Related parameters
Micro texture	<0.5mm		aggregate	skid resistance
Macro texture	0.5mm – 5cm	0.1mm – 2.0cm	aggregate and mortar	macro texture depth, mean profile depth
Mega texture	5cm – 50cm	0.1mm – 5.0cm	potholes, waviness	texture profile level
Irregularity	>50cm		structural integrity, foundations	ISO 8608:2016 [10] road classes, waviness, IRI

Several spectral texture standards are in place. The texture profile level is the amplitude spectrum of the longitudinal road profile in third octave bands [9]. On the other hand, for irregularity up to 90m, ISO 8608:2016 defines road quality classes A-F based on the peak spectral density of the road profile [10]. For instance, irregularity must be smooth to accommodate high velocity traffic (classes A and B) [11]. On the other hand, for local roads, irregularity is less important, while roads classified as F are mostly unpaved. There is quite some discussion on whether the parameters listed in ISO 8608:2016 reflect the

actual road profiles [11]. On the other hand, the European Committee for Standardization defines numerical methods to predict the ISO 8608:2016 road surface class, given the road profile [12].

Several single value indicators are also defined, which are based on the road profile and construction materials. For instance, skid resistance is defined as the ratio of the horizontal friction of the surface to the vertical load force [13]. Skid resistance is mostly related to the micro texture of the road. As an example: frequent traffic polishes micro texture which results in a decrease in skid resistance. Macro texture is related to water draining and wet roads also cause a decrease in skid resistance.

Another standard measure is the international roughness index (IRI) measured in m/km [14]. IRI is the relative velocity between the axle and the sprung mass of a reference car. The golden car model is a quarter car model with parameters related to the reference car. This model includes a stiffer suspension, in order to decrease the amount of resonances in the model. In addition, this property can be calculated from the power spectral density roughness as there exists a linear correlation between the two [14].

Moreover, a mean profile depth (MPD) is defined by ISO 13473-1:2019 [15], which is only related to the macro texture. MPD is the average value of the height difference between the profile and a horizontal line through the highest peak (the peak level) over a 100mm long baseline in a macro texture range.

A final ISO measure is a dynamic load coefficient (DLC) [16]. DLC is defined as the standard deviation of the dynamic forces in a whole-body to the static forces. DLC focusses on comfort for humans in vibrations and low frequency sound. Vibrations from 0.1Hz to 0.5Hz relate to motion sickness, while on the other hand, vibrations from 0.5Hz to 80Hz are relevant for health, comfort and perception.

Based on this discussion, it can be expected that the proposed opportunistic sensing would be suitable to estimate road quality classes, IRI, DLC, and to a lesser extend texture profile level, but that it is probably not informative for MPD and skid resistance.

3. Methodology

As computation power, data storage, and wireless data transfer are decreasing in cost, opportunistic sensing and big data is on the advent. In addition, a landscape of open source software frameworks (Pandas, TensorFlow, NumPy, SciPy, scikit-learn, etc.) provide the scientific community with the necessary tools to utilize big data, machine learning and artificial intelligence algorithms.

In this paper, an opportunistic approach is proposed: equipping cars that are on the road for other purposes with noise and vibration sensors to assess road quality. For this, sensor boxes equipped with a microphone, a tri-axial accelerometer and a GPS sensor are put in the trunk of the fleet of cars. Using 3G connection, acquired data is transferred to the analysis server.

The response of the tire/car combination to the road surface texture depends on the spatial wavelength and the driving speed. To cover the range of interest (**Error! Reference source not found.**), acceleration is measured from 1Hz to 40Hz, while sound is collected from 25Hz to 4kHz. Third octave band spectra are calculated at 50Hz sampling rate and used to determine statistical indicators such as mean, median, percentile-values and equivalent level over one-second intervals. Vibration (17 values) and sound spectrum (23 values) are concatenated into a combined spectrum L containing 37 third octave bands. A linear weighting method is applied for the three overlapping bands.

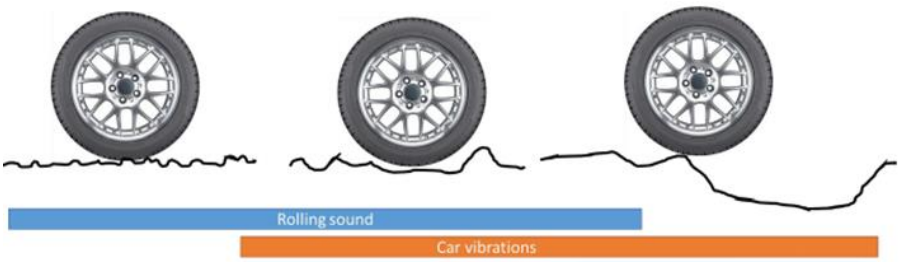

Figure 2: Relationship between rolling noise and car vibrations to the road profile.

3.1 Pavement texture

In this section, the relative texture profile level $dT(i,\lambda)$ [dB] is introduced which represents the deviation from the average road profile in the study area at a spatial wavelength λ [m]. In this study, the spatial wavelength λ ranges from 1cm to 10m expressed in third octave bands. The combined vibration and sound spectrum $L(i,c,t,f)$ [dB], defined by third octave bands from 1Hz to 4kHz, is measured per car *c*, on road segment *i*, during trip *t* and at the centre frequency f. This spectrum is used to make an estimate $dT'(i,\lambda)$ [dB] of the relative pavement texture profile. Moreover, each trip represents a moment in time and a dependency of the current situation in and around the car (e.g. music, engine noise, passengers and other cars on the road). In addition, *v(t)* [m/s] is a measure of the instantaneous speed obtained each second from the GPS sensor.

3.1.1 Removing known dependencies

The two most important modifiers: car transfer function and dependence on driving speed are then removed from the measurements. For this work, the car transfer function, $H_c(f)$ [dB], is assumed to relate the excitation of the tire at frequency *f* to the measurement inside the car. Using a transfer function implies linearity and time invariance, which is not necessarily the case. Hence, we expect a rather poor model, especially for the phase, and thus we opt for using only the magnitude of H_c averaged over third octave bands. Since H_c cannot be easily determined for the fleet of cars participating in the opportunistic sensing, it is approximated by for the *N* the amount of samples taken:

$$\boldsymbol{H_c(f) \approx H'_c(f) = \frac{1}{N}\sum_t L(i(t), c, t, f).} \quad (1)$$

This approximation relies on the hypothesis that the tire excitation will be close to white noise if a random sample of the distribution of road surfaces, driving styles and speeds is taken. In this paper, the first three hours of driving faster than 30 km/h and slower than 125 km/h for vibrations are selected. For sound, the first three hours of driving with speed ranging between 50 km/h and 125 km/h are used.

Using Eq. (2) we can define $T'(i,c,t,\lambda)$ which is the approximation of $T(i,\lambda)$, i.e. the actual surface texture of the road in dB:

$$\boldsymbol{T'(i,c,t,\lambda) = L\left(i,c,t,\frac{v(t)}{\lambda}\right) - H'_c(c,\frac{v(t)}{\lambda}) \approx T(i,\lambda).} \quad (2)$$

Note that T' selects the frequency band $v(t)/\lambda$ of the combined spectrum L. Doing so, this selects the sound or vibration band for which the current surface wavelength λ produces excitement. It is thereby assumed that the tire is an infinitesimal point (in contrast to the real tire) and therefore, vertical accelerations (and sound) are directly related to the height of the road surface texture at that frequency.

Driving speed not only determines the frequency of tire excitation but also the strength of this excitation. This is a main reason for remaining variance amongst the approximations *T'* over cars and trips. For example, the rolling noise level typically shows a power law dependence that depends on tire treat and road surface type [17]. However, the proposed model ignores explicit dependence on road type and assumes a more general driving speed dependence. Hence, the driving speed dependence for each car – and tire type – can be obtained for the average roads that the car has been driving on. By subtracting from the approximation *T'*, an approximation for the relative texture profile level dT' can be obtained as:

$$\boldsymbol{dT'(i,c,t,\lambda) = T'(i,c,t,\lambda) - GAM_{T'}(v(t),c,\lambda).} \quad (3)$$

There, GAM_T, is a Gaussian additive model function eliminating remaining effects of the speed from the equation. GAM_T, is then fitted on T' with varying speeds (30 minutes of driving in 0-30, 30-50, 50-70, 70-90 and 110-130 km/h ranges). Finally, $dT'(i,\lambda)$ for each road segment is obtained by averaging over all cars and all trips that pass that road segment hereby assuming that these are independent observations.

3.1.2 Calibration with the laser profiler

To translate the relative texture profile level to a quantified texture profile levels, a calibration step is performed using laser profiling measurement conducted by the Belgian Road Research Institute (BRRI). The laser equipment is expected to be accurate for wavelengths lower than 1m. On the other hand, the opportunistic approach is expected to be applicable only for λ above 2cm because the tire is expected to filter out micro and macro texture, while at the same time the air-pumping effects are more related to this spatial texture range. Thus, the useful range for calibration lies between 2cm and 1m.

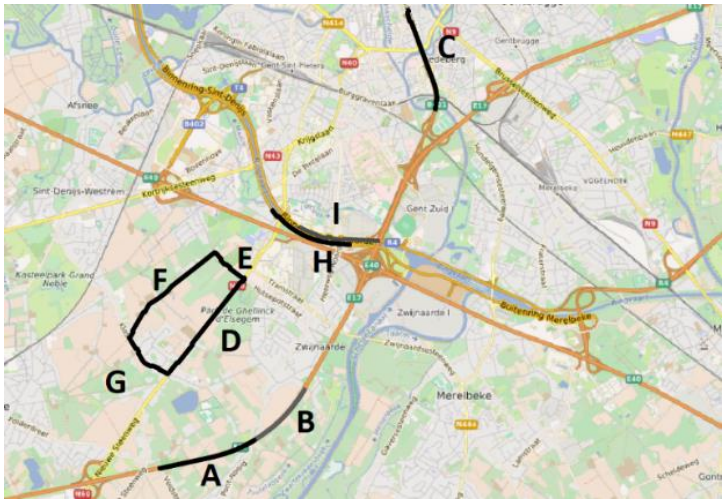

Figure 3: Road sections in Gent, Belgium measured with laser profiler and used for calibration of the road texture profile levels measured using opportunistic sensing.

During the dry weather in winter 2018/2019, a calibration run with a laser profiler vehicle has been performed. Several trajectories shown in Figure 3 have been chosen to accommodate a wide variety of pavement materials and degradation (new/worn). Simultaneously, three cars with the sensor box installed followed the laser profiler vehicle: car 1 – Kia Niro (hybrid engine gasoline/electric, year 2018), car 2 – Volvo XC90 (gasoline, year 2018) and car 3 – Peugeot 406 (diesel, older than 10 years). During a first passage on the calibration run, car 1 drove electric therefore no combustion engine noise was present. On the other hand, during the second passage, the gasoline engine was turned on for car 1. The laser profiler was mounted on the backside of measurements car near the right rear tire. Using the laser profiler contactless method [15], a single line was traced sampling every millimeter.

Statistics on the profiler need to be taken over longer stretches of road to account for the variations due to one-dimensional trace. In literature, statistics are calculated over lengths of 100m [18-19], 152.4m [20] and even 1000m and are used for measuring irregularity of roads. In this paper, the laser data were processed to third octave band texture profile levels in dB(µm), $T_l(i,\lambda)$, with the spatial index *i* referring to 20m intervals that roughly coincided with the segments used in the opportunistic sensing approach. Due to the poor spatial match, regression analysis on the 20m interval data could not be used for calibration, hence the approximate texture level $T''(i,\lambda)$ is defined:

$$\boldsymbol{T''(i,\lambda) = (dT'(i,\lambda) - \mu')\,\sigma_l/\sigma' + \mu_l}\,. \tag{4}$$

Quantities μ_l, σ_l, μ' and σ' in Eq. (4) are defined using Eqs. (5)-(6), while *N* represents the number of overlapping segments:

$$\boldsymbol{\mu_l(\lambda) = \frac{1}{N}\sum T_l(i,\lambda);\ \sigma_l(\lambda) = \sqrt{\frac{1}{N}\sum_i (T_l(i,\lambda) - \mu_l(\lambda))^2}} \tag{5}$$

$$\boldsymbol{\mu'(\lambda) = \frac{1}{N}\sum dT'(i,\lambda);\ \sigma'(\lambda) = \sqrt{\frac{1}{N}\sum_i (dT'(i,\lambda) - \mu'(\lambda))^2}} \tag{6}$$

3.2 Noisiness index

In previous work [6], the same opportunistic sensing has been used to label roads according to their noisiness. A noisiness index was defined as the sum over the frequency range 350Hz till 1250Hz of the relative noise level:

$$\boldsymbol{dL_i(f,i) = \frac{1}{N}\sum_{t,c} dL(f,i,t,c), \text{ for } t,c|v(t,i) \in \left[v_{i,85}, v_{i,lim}\right]} \quad (7)$$

The relative noise level dL in Eq. (7), is calculated using an equation similar to Eq. (3).

4. Results and discussion

Fig. 4 shows the longitudinal road texture spectrum averaged over each of the segments represented in Figure 3. The graph on the left presents the opportunistic sensing measurements T'' (Eq. (4)), while the laser measurements T_l are displayed on the right. As explained before, above a spatial frequency of about 30cycles/m the results obtained from opportunistic sensing could not be trusted. It can clearly be seen that the texture determined from the laser measurements is more similar between roads or even crosses at higher spatial frequencies, while this is not the case for T''. One could indeed expect a reverse dependence of sound on texture at these frequencies due to air pumping. At λ equal to 1m, a peak is visible in both results (due to μ_l (1m)) which could be amplified by the laser measurement car dynamics.

Considering the individual segments, several observations can be made. The outlier trajectory of segment E, which consist of concrete plates, is obvious in both spectra. Moreover, due to the painted cycle lane in this segment, the laser that samples a single line only, records a smoother pavement at the higher frequencies while this is not visible in the opportunistic sensing approach which samples both wheel tracks. Trajectory G is a local road with a new SMA and thus has a smooth macro texture but at the same time it has a higher irregularity than the highway segments. Trajectory D is a worn DAC which shows a higher amplitude in the macro texture range in both measurement models (the aggregate becomes lose). Trajectory I, a worn concrete, shows a high macro texture for both measurement methods. The largest differences between both methods in the range 2 to 30cycles/m are found for the highways. In particular, for trajectories A and B, opportunistic method overestimates the mega texture while for trajectory C it underestimates the mega texture. It should be noted that trajectory C differs from general highway pavement, since this is a viaduct with a lot of bridge joints at set distances. As explained by Múčka et al. [11], high-speed highways require smooth surfaces, in irregularity texture range.

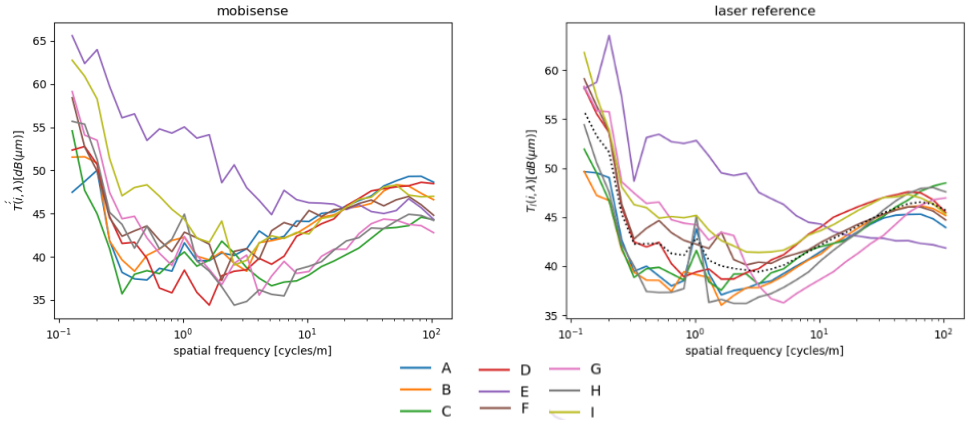

Figure 4: Left: results of calibrated opportunistic measurements $\boldsymbol{T''(i,\lambda)}$ (Eq. (4)), right: reference laser measurements $\boldsymbol{T_l(i,\lambda)}$. Both are averaged over all segments $\boldsymbol{i}$ per segments defined in Fig. 3. The dotted black line on the right graph represents $\boldsymbol{\mu_l}$ (Eq. (5)).

Maps of selected third octave bands (Figure 5) of road texture level shed some light on different aspects of the state of the road. Mega texture (0.1m and 0.5m wavelengths are shown) gives an indication

of wear, but also identifies cobblestone pavement that are used for some of the inner-city roads in Ghent. Waviness (2.5m wavelength is shown) may indicate problems with the road's foundation but it is also systematically found on roads such as the ring road around the city. Fig. 5 also shows the noisiness classes. As expected, visual inspection of the maps shows that noisiness is higher for the road segments with high amplitude mega texture.

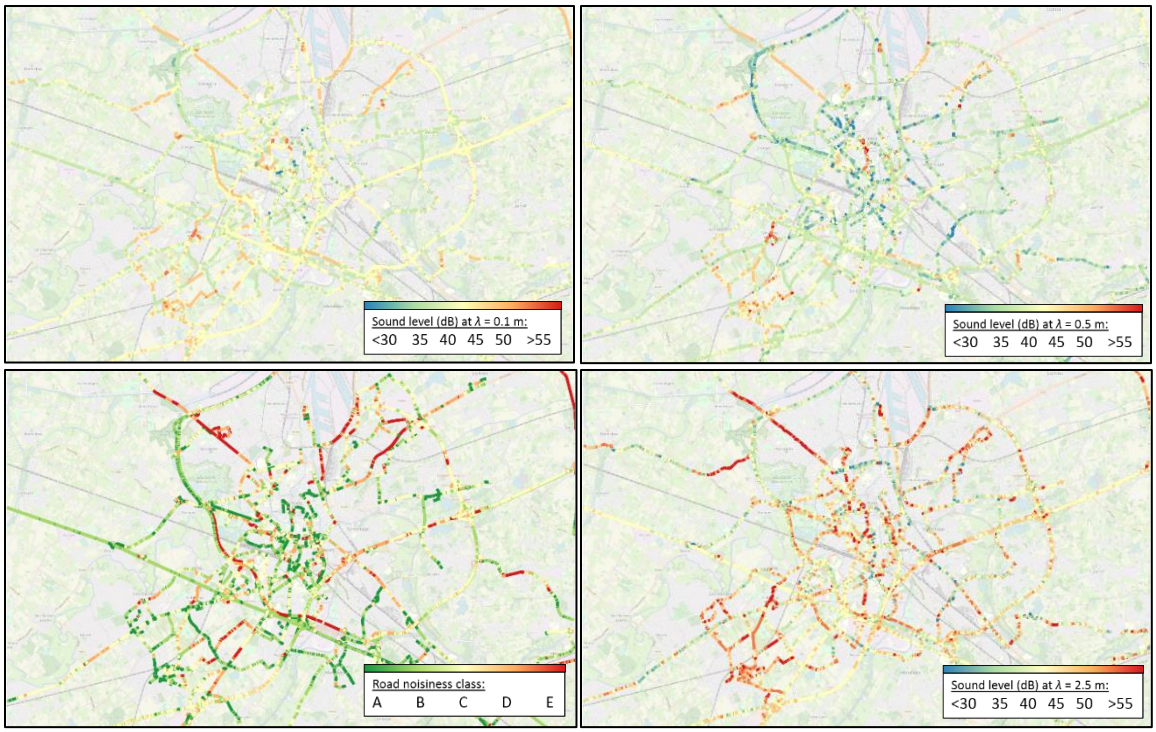

Figure 5: Spatial representation of the pavements using opportunistic sensing measurements around the city of Ghent (clockwise from top right): level at $\boldsymbol{\lambda = 0.1\mathbf{m}}$, level at $\boldsymbol{\lambda = 0.5\mathbf{m}}$, level at $\boldsymbol{\lambda = 2.5\mathbf{m}}$, road nosiness class.

5. Conclusion and outlook

This paper shows that the opportunistic sensing of noise and vibration using many cars allows to estimate the road texture level quite accurately even when a very simple model for relating it to the measured quantities is used. Nevertheless, this comparison is done using the data obtained in good driving conditions: the car audio system was not in use and the drivers and passengers were not talking. Moreover, it can be assumed that during the test drive, the engine was not strongly loaded by the fast acceleration or high driving speeds as the speed was kept constant. Thus, future research on removing confounders would still be needed. Finally, more precise models for relating the measurements to texture level may allow to extend the measurement range to lower and higher spatial wavelengths.

6. Acknowledgements

This work was performed within the framework of the ICON project MobiSense (grant No. HBC.2017.0155), supported by IMEC and Flanders Innovation & Entrepreneurship (Vlaio).

REFERENCES

1. Sandberg, U. and Descornet, G. Road surface influence on tire/road noise, *Proceedings of the International conference on noise control engineering (Inter noise 80)*, Miami, USA, 8-10 December, (1980).

2. Cantisani, G. and Loprencipe, G. Road roughness and whole body vibration: Evaluation tools and comfort limits, *Journal of Transportation Engineering*, **136** (9), 818-826, (2010).
3. Lercher, P. Environmental noise and health: An integrated research perspective, *Environment international*, **22** (1), 117-129, (1996).
4. *Roadroid.* [Online.] available: https://www.roadroid.com/Home/About
5. Van Geem, C., Bellen, M., Bogaerts, B., Beusen, B., Berlémont, B., Denys, T., De Meulenaere, P., Mertens, L. and Hellinckx, P. Sensors on Vehicles (SENSOVO): Proof-of-concept for Road Surface Distress Detection with Wheel Accelerations and ToF Camera Data Collected by a Fleet of Ordinary Vehicles, *Transportation Research Procedia*, **14**, 2966-2975, (2016).
6. David, J., Van Hauwermeiren, W., Dekoninck, L., De Pessemier, T., Joseph, W., Filipan, K., De Coensel, B., Botteldooren, D. and Martens, L. Rolling-noise-relevant classification of pavement based on opportunistic sound and vibration monitoring in cars, *48th International Congress and Exhibition on Noise Control Engineering (Inter.noise 48)*, Madrid, Spain, 16-19 June, (2019).
7. ISO 10844:2014. Specification of test tracks for measuring noise emitted by road vehicles and their tyres. *International Organization for Standardization*, (2014).
8. Laurent, J., Talbot, M. and Doucet, M. Road surface inspection using laser scanners adapted for the high precision 3D measurements of large flat surfaces, *Proceedings of International Conference on Recent Advances in 3-D Digital Imaging and Modeling*, Ottawa, Ontario, Canada, 303-310, (1997).
9. ISO 13473-2:2002. Characterization of pavement texture by use of surface profiles. Part 2: Terminology and basic requirements related to pavement texture profile analysis (confirmed in 2018), *International Organization for Standardization*, (2002).
10. ISO 8608:2016: Mechanical vibration: Road surface profiles and Reporting of measured data, *International Organization for Standardization*, (2016).
11. Múčka, P. Simulated Road Profiles According to ISO 8608 in Vibration Analysis, *Journal of Testing and Evaluation*, **46**(1), 1-14, (2019).
12. CEN-PREN 13036-5. Road and Airfield Surface Characteristics – Test Methods, Part 5: Determination of Longitudinal Unevenness Indices, *European Committee for Standardization (CEN)*, Brussels, Belgium, (2015).
13. Asi, I. M., Evaluating skid resistance of different asphalt concrete mixes, *Building and Environment*, **42** (1), 325-329, (2017).
14. Sun, L., Zhang, Z. and Ruth, J. Modeling indirect statistics from surface roughness, *Journal of Transportation Engineering*, **127** (2), 105-111, (2001).
15. ISO 13473-1:2019. Characterization of pavement texture by use of surface profiles. Part 1: Determination of mean profile depth, *International Organization for Standardization*, (2019).
16. ISO 2361-1:1997. Mechanical vibration and shock: Evaluation of human exposure to whole-body vibration. Part 1: General requirements (rev. 2017), *International Organization for Standardization*, (1997).
17. Winroth, J., Kropp, W., Hoever, C., Beckenbauer, T. and Männel, M. Investigating generation mechanisms of tyre/road noise by speed exponent analysis, *Applied Acoustics*, **115**, 101-108, (2017).
18. Nagel, M., Maerschalk, G. and Schneider, B.Variabilitätsuntersuchung der Rohdaten zur Stabilisierung der Ableitung abschnittsbezogener Zustandsgrößen für die Bewertung der Fahrbahnbefestigungen der Bundesfernstraßen [Variability analysis of the raw data for the stabilization of the derivative section related state variables for evaluating the pavements of the federal roads], Projekt-Nr. 29.0178/2007/BMVBS, SAP Maerschalk, Munchen, Germany, (2008).
19. Braun, H. and Hellenbroich, T. Results of road roughness measurement in Germany, VDI-Berichte Nr. 877, VDI-Verlag, Düsseldorf, Germany, 47–80, (1991).
20. Múčka, P. and Kropáč, O. Properties of random component of longitudinal road profile influenced by local obstacles, *International Journal of Vehicle Systems Modelling and Testing*, **4**(4), 256–276, (2009).

Proceedings of
the 26th International Congress on Sound and Vibration

Montreal bridges, 2019

Edited by:

ICSV26 Local Committee in Montreal

ISSN 2329-3675
ISBN 978-1-9991810-0-0

Published by: Canadian Acoustical Association